

## ACCEPTED VERSION

Solmaz Saboohi, Hans J. Griesser, Bryan R. Coad, Robert D. Short and Andrew Micheltore

### Promiscuous hydrogen in polymerising plasmas

Physical Chemistry Chemical Physics, 2018; 20(10):7033-7042

This journal is © the Owner Societies 2018

Published at: <http://dx.doi.org/10.1039/C7CP08166A>

#### PERMISSIONS

<http://www.rsc.org/journals-books-databases/journal-authors-reviewers/licences-copyright-permissions/#deposition-sharing>

### Deposition and sharing rights

When the author accepts the licence to publish for a journal article, he/she retains certain rights concerning the deposition of the whole article. This table summarises how you may distribute the accepted manuscript and version of record of your article.

Sharing rights	Accepted manuscript	Version of record
Share with individuals on request, for personal use	✓	✓
Use for teaching or training materials	✓	✓
Use in submissions of grant applications, or academic requirements such as theses or dissertations	✓	✓
Share with a closed group of research collaborators, for example via an intranet or privately via a <a href="#">scholarly communication network</a>	✓	✓
Share publicly via a scholarly communication network that has signed up to STM sharing principles	⌚	✗
Share publicly via a personal website, institutional repository or other not-for-profit repository	⌚	✗
Share publicly via a scholarly communication network that has not signed up to STM sharing principles	✗	✗

⌚ Accepted manuscripts may be distributed via repositories after an embargo period of 12 months

15 October 2019

<http://hdl.handle.net/2440/114140>

# Promiscuous hydrogen in polymerising plasmas

Solmaz Saboohi<sup>1</sup>, Hans J. Griesser<sup>1</sup>, Bryan R. Coad<sup>1,2</sup>, Robert D. Short<sup>3</sup>, Andrew Michelmore<sup>1,4\*</sup>

1. *Future Industries Institute, University of South Australia, Mawson Lakes, South Australia 5095, Australia*
2. *School of Agriculture, Food and Wine, University of Adelaide, Adelaide SA 5005, Australia*
3. *Materials Science Institute and Department of Chemistry, University of Lancaster, City of Lancaster, UK*
4. *School of Engineering, University of South Australia, Mawson Lakes, South Australia 5095, Australia*

\* Corresponding author:

Email: [andrew.michelmore@unisa.edu.au](mailto:andrew.michelmore@unisa.edu.au)

## Abstract

Historically, there have been two opposing views regarding deposition mechanisms in plasma polymerisation, radical growth and direct ion deposition, with neither being able to fully explain the chemistry of the resultant coating. Deposition rate and film chemistry are dependent on the chemistry of the plasma phase and thus the activation mechanisms of species in the plasma are critical to understanding the relative contributions of various chemical and physical routes to plasma polymer formation. In this study, we investigate the roles that hydrogen plays in activating and deactivating reactive plasma species. Ethyl trimethylacetate (ETMA) is used as a representative organic precursor, and additional hydrogen is added to the plasma in the form of water and deuterium oxide. Optical emission spectroscopy confirms that atomic hydrogen is abundant in the plasma. Comparison of the plasma phase mass spectra of ETMA/H<sub>2</sub>O and ETMA/D<sub>2</sub>O reveals that 1) proton transfer from hydronium is a common route to charging precursors in plasma, and 2) hydrogen abstraction (activation) and recombination (deactivation) processes are much more dynamic in the plasma than previously thought. Consideration of the roles of hydrogen in plasma chemistry may then provide a more comprehensive view of deposition processes and bridge the divide between the two disparate schools of thought.

## Introduction

Many questions have been raised regarding plasma polymers due to seemingly contradictory observations which have thwarted the development of a unified mechanistic theory of deposition. For example, why are plasma polymers always depleted in hydrogen,<sup>1</sup> why do they auto-fluoresce due to double bonds even when the precursor is saturated,<sup>2</sup> why do they age due to dangling bonds,<sup>3,4</sup> and why does plasma polymer chemistry correlate with ion chemistry in some cases,<sup>5</sup> but with neutral chemistry in others<sup>6,7</sup>? These questions cannot be explained exclusively by either radical or ionic growth mechanisms, and detailed understanding of these processes has remained elusive despite reports dating back to the 1960s.<sup>8-10</sup>

Plasma polymer coatings can be used to tailor surface properties<sup>11</sup> including chemical functionality,<sup>12,13</sup> wettability<sup>14</sup> and modulus,<sup>1,15</sup> without affecting bulk properties, and thus have found application in solar cells,<sup>16</sup> microelectronics,<sup>17</sup> diamond-like carbon (DLC) coatings,<sup>18</sup> polymer brush grafting,<sup>19</sup> slow release coatings<sup>20,21</sup> and protein separation<sup>22</sup>. However, due to a lack of detailed knowledge of deposition mechanisms, industrial uptake in many cases has proceeded based on empirical trial-and-error rather than predictive modelling.<sup>23</sup> This is because the gas phase of plasmas are extremely complex and there are multiple routes for deposition to occur; direct ion deposition<sup>24</sup>, plasma radical – surface radical combination<sup>25</sup> and radical propagation<sup>13</sup>. Direct ion deposition occurs when positive ions are accelerated to negatively charged surfaces in contact with the plasma.<sup>26</sup> The kinetic energy with which the ions collide is typically 10-30eV, which enables a number of surface interactions, including scattering, dissociative chemisorption, soft-landing and abstraction.<sup>27</sup> The dissipation of this kinetic energy is also capable of causing bond scission between atoms already on the surface resulting in surface radical formation.<sup>28</sup> These surface radicals then facilitate the radical combination and radical propagation deposition mechanisms. Radical combination requires the production of plasma phase radicals, while radical propagation requires plasma species with double bonds.

The relative contributions of these mechanisms are crucial in determining the rate of deposition and the retention of chemical functionality.<sup>29</sup> Deposition via radical combination can lead to poor functional retention as precursor fragmentation is a prerequisite for this mechanism. Ionic deposition can also suffer from plasma phase fragmentation, but additionally from surface etching and atomic rearrangement, although we have recently shown that highly functionalised plasma polymer films were formed from intact protonated precursor ions via the plasma  $\alpha$ - $\gamma$  transition<sup>5,30</sup>. It has also been shown that radical propagation via double bonds inherent in the

precursor structure can lead to high functional retention as intact precursor molecules represent the vast majority of the species in the plasma.<sup>31</sup> In most cases the degree of functional retention is maximised by using very low RF power inputs to minimise fragmentation, but this may require a trade-off for other properties such as solubility or modulus.

Thus, how ions, radicals and double bonds are formed and behave in the plasma is crucial to understanding deposition processes. Gas phase abstraction of hydrogen is well known<sup>32-34</sup> and additionally it has previously been hypothesized that precursor protonation occurs via proton exchange from hydronium<sup>35</sup>, however experimental evidence is lacking. Hydrogen therefore plays key roles in producing plasma ions and radicals, but the degree to which these mechanisms determine plasma chemistry is unknown and is the focus of this study. Ethyl trimethylacetate (ETMA) is used as a representative organic precursor, and additional hydrogen is added to the plasma in the form of water (H<sub>2</sub>O) or deuterium oxide (D<sub>2</sub>O). Optical emission and plasma phase mass spectra are used to measure the properties of the neutral and ionic species in the plasma phase. Comparison of the mass spectra results for ETMA/H<sub>2</sub>O and ETMA/D<sub>2</sub>O plasmas reveals the crucial role hydrogen plays in determining plasma chemistry.

## **Experimental section**

### **Materials**

Ethyl trimethylacetate (ETMA, Pt no. 234559, 99% purity) and Deuterium oxide (D<sub>2</sub>O, Pt no. 151882, 99.9% atomic D) were sourced from Sigma-Aldrich, D<sub>2</sub>O. H<sub>2</sub>O used was Milli-Q water.

**Plasma Polymerisation.** Plasma mixtures of ETMA, H<sub>2</sub>O and D<sub>2</sub>O were created using a stainless steel vacuum chamber. The plasma reactor used has been described and characterized elsewhere.<sup>36</sup> The chamber was pumped down by a two-stage rotary pump with an in-line liquid nitrogen trap to reach a base pressure below 0.002 mbar, and the ETMA, H<sub>2</sub>O and D<sub>2</sub>O, placed in separate flasks, were degassed by freeze-thaw cycling with liquid nitrogen. The partial pressures of ETMA, H<sub>2</sub>O and D<sub>2</sub>O in the chamber were controlled by separate needle valves (Chell, UK). Plasma was ignited using an RF power generator (13.56 MHz, RFG050 Coaxial Power Systems, UK) with a matching network (AMN150, Coaxial Power Systems, UK). Air plasma was used to etch the reactor prior to each experiment for 30 min. Gas mixtures of ETMA:D<sub>2</sub>O and ETMA:H<sub>2</sub>O with ratio of 1:1 (partial pressures of 0.03mbar : 0.03 mbar) , 1:2

(partial pressures of 0.02mbar: 0.04 mbar) and 2:1 (partial pressures of 0.04mbar: 0.02 mbar) were used such that the total gas pressure remained constant at 0.06 mbar.

**Plasma Mass Spectrometry (MS).** A quadrupole mass spectrometer (Hiden EQP1000 energy resolving mass spectrometer) was mounted along the reactor midline axis. The system was differentially pumped during operation using a turbomolecular pump. The internal pressure remained below  $5 \times 10^{-7}$  mbar. A grounded 100  $\mu\text{m}$  orifice was used during sampling. The mass spectrometer was operated in positive ion and residual gas analysis (RGA) modes. In RGA mode, the neutral species entering the instrument were charged by electron impact using an electron gun operated at 70eV and 10mA. In positive ion mode, the ion optics were first tuned to the peak ion energy at each power for the protonated precursor by acquiring the ion energy distribution. The positive ion mass spectra were then collected at this peak ion energy in the range 0–300 m/z. The spectra were corrected for instrument transmission assuming the peak intensity was proportional to  $m^{-1}$ , as advised by the manufacturer.

### **Optical Emission spectroscopy (OES)**

An Ocean optics HR4000 spectrometer was used to detect the optical emission spectra generated by the various plasmas tested. Radiation was collected using a collection lens attached to an optical fibre placed outside of a window in the plasma chamber. Chamber windows were shielded to exclude ambient light from being detected. Spectra were collected from 200-1100 nm with a resolution of  $\sim 1\text{nm}$ . Spectra were collected using Ocean Optics Spectra Suit software and were time-averaged over 2secs.

### **Results**

The chemistry of the plasma phase was measured using both OES and MS. It should be noted that OES probes the bulk of the plasma, while MS probes the species which arrive at surfaces in contact with the plasma. Therefore signals detected by OES are the result of plasma phase reactions, and represent the chemistry of the bulk plasma phase. Species measured by MS are formed in the bulk of the plasma, but may have then undergone multiple surface interactions/collisions before being detected. MS results therefore characterise the chemistry of species arriving at surfaces which are responsible for deposition processes.

### **Optical Emission Spectra (OES) of ETMA plasma**

OE Spectra of the ETMA plasma were recorded at applied RF powers of 25 W and 40W at a gas pressure of 0.06 mbar and are presented in Fig 1. 0.06 mbar was chosen as this is near the  $\alpha$  to  $\gamma$  plasma transition which results in increased plasma density for a given power input and thus maximises the signal to noise ratio<sup>5</sup>.

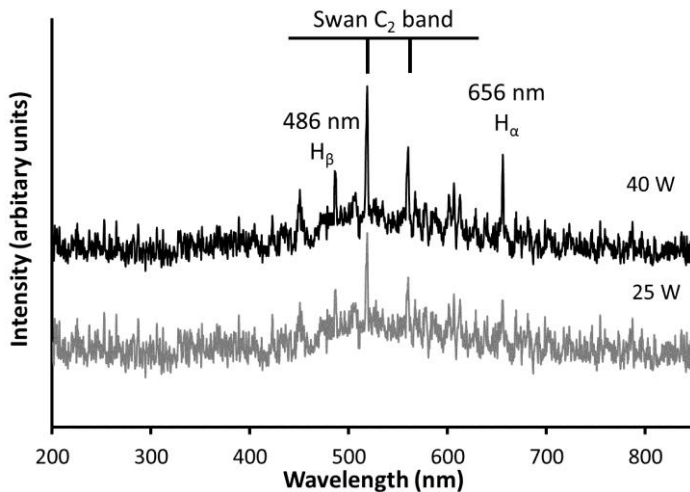


Figure 1 Optical Emission Spectra of ETMA plasma at 0.06 mbar.

As expected, typical carbonaceous species lines following the C<sub>2</sub> Swan system (A<sub>3</sub>Π → X<sub>3</sub>Π, 450 nm–600 nm) are clearly present in the visible range.<sup>37</sup> The strongest of these are the Swan band systems at 516.52, 563.55nm, with smaller peaks at 440nm, and a triplet at ~600nm. The minor peak at 773nm is assigned to emission from CH<sub>x</sub>. Figure 1 clearly indicates that in addition to the carbonaceous species lines, there exist peaks at 656.3 and 486.2nm which become more intense at high power. These correspond to the hydrogen Balmer lines, H<sub>α</sub> (n<sup>2</sup>=3→2, 656.3nm) and H<sub>β</sub> (n<sup>2</sup>=4→2, 486.2nm), indicating the presence of atomic hydrogen in the plasma phase. Hydrogen molecular lines have much lower intensities due to the high degree of H<sub>2</sub> dissociation but radiate quite weakly throughout the entire visible spectrum, but most intensely around 600 nm.<sup>38</sup> Calculating the relative densities of atomic H and molecular H<sub>2</sub> from these spectra is fraught, as the cross-sections vary dramatically with electron temperature<sup>39</sup>, however the peaks observed show that both are certainly present in the plasma phase.

### OES H<sub>2</sub>O plasma

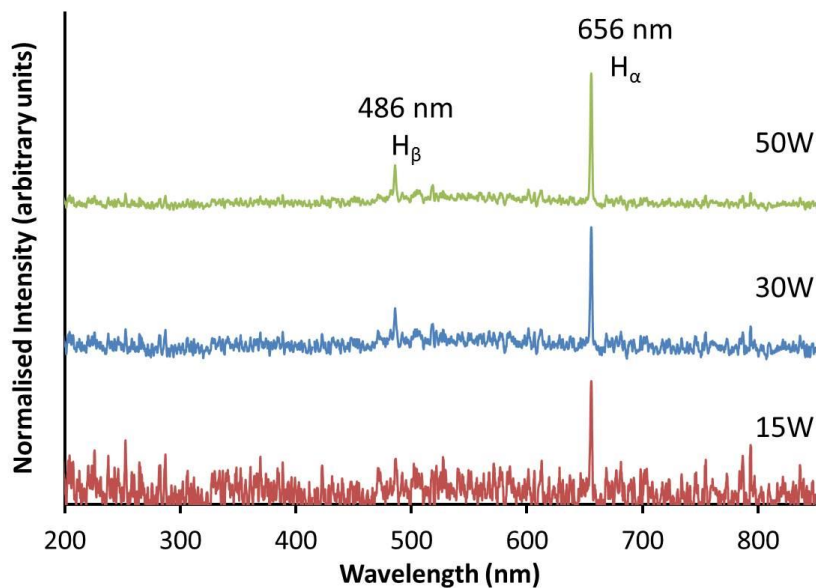


Figure 2. Optical Emission Spectra of H<sub>2</sub>O plasma

Figure 2 shows the optical emission spectrum of H<sub>2</sub>O plasma at 0.03 mbar. The H<sub>α</sub> and H<sub>β</sub> peaks at 655.3 and 486nm are again observed, but without the C<sub>2</sub> Swan series bands observed for ETMA plasma. Also, the broad background observed for ETMA plasma between 450 and 600nm is not observed which is associated with the formation of molecular hydrogen H<sub>2</sub>, and no peaks associated with molecular oxygen were observed. D<sub>2</sub>O plasma showed the same series of peaks as the difference between the H<sub>α</sub> and D<sub>α</sub> peaks is ~0.17nm which is below the resolution of the HR4000, so the Balmer peaks for H• and D• are not resolvable.

## Neutral Mass Spectrum of ETMA plasma

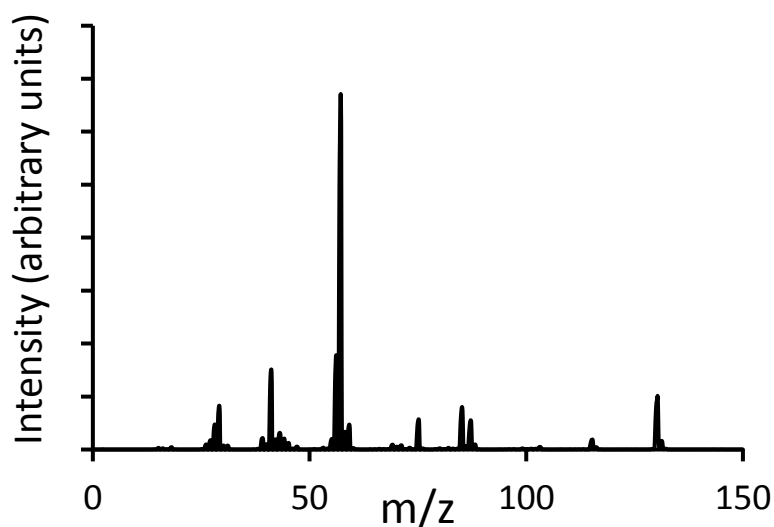


Figure 3. Residual Gas Analysis spectrum of ETMA plasma at 0.06 mbar at 10W

The neutral mass spectrum of ETMA plasma is shown in Figure 3. The peak at 130 m/z corresponds to the precursor after charging via electron impact. Peaks associated with scission of C-C and C-O bonds are present, including loss of methyl groups (115 m/z), ethoxy groups (85 m/z) and the tert-butyl group (57 m/z). Peaks associated with small hydrocarbon species ( $C_2H_5^+$ , 29m/z and  $C_3H_5^+$ , 41m/z) are also observed. No peaks with mass greater than the precursor are evident. Thus, electron impacts with neutral molecules give rise to ionic radicals via bond scission and removal of an electron.

## Positive Ion Mass Spectrometry

### ETMA/H<sub>2</sub>O

Figure 4 shows the positive ion mass spectra of a (1:1) mixture of ETMA mixture with H<sub>2</sub>O at a plasma input power of 10W and total pressure of 0.06 mbar.



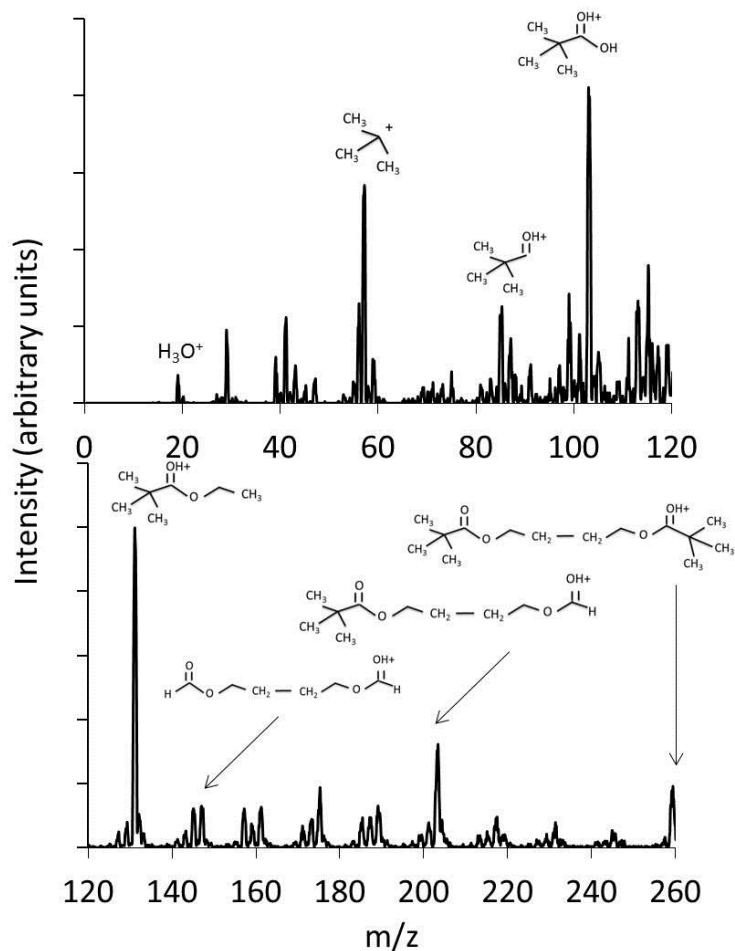
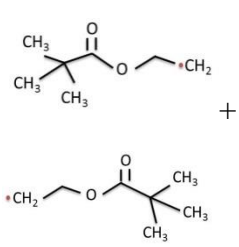
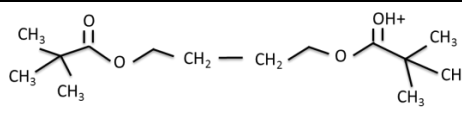
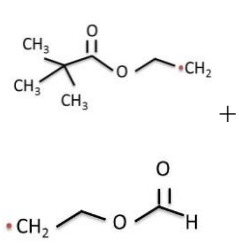
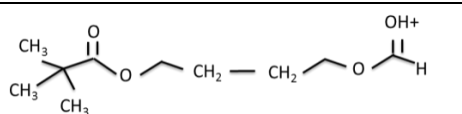
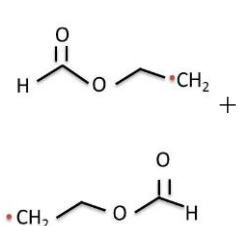
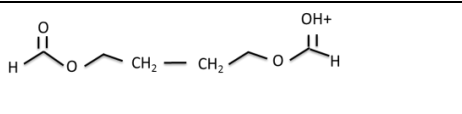


Figure 4 Positive ion mass spectrum of ETMA/H<sub>2</sub>O plasma at 0.06 mbar and 10W

Table 1 Assignment of precursor and fragment mass spectrum peaks for ETMA plasma.

Positive Ion Mass (m/z)	Putative Positive Ion Fragment Structure
131	<chem>CC(C)(C)OC[OH+]</chem>
103	<chem>CC(C)(C)O[OH+]</chem>
87	<chem>CC(C)(C)[OH+]</chem>
57	<chem>CC(C)[+]</chem>

Table 2 Assignment of oligomer mass spectrum peaks for ETMA plasma.

Reactants	Positive Ion Mass (m/z)	Putative Positive Ion Oligomer Structure
$129 + 129 + \text{H}^+$ 	259 245 – methyl + H• 231 – 2 methyl + 2H• 217 – 3 methyl + 3H•	
$129 + 73 + \text{H}^+$ 	203 189 – methyl + H• 175 – 2 methyl + 2H• 161 – 3 methyl + 3H•	
$73 + 73 + \text{H}^+$ 	147	

The spectrum shows a peak corresponding to the protonated precursor molecule  $[\text{M}+\text{H}]^+$  at  $m/z$  131 in agreement with previously reported positive ion mass spectra for other precursors.<sup>31</sup> Additionally, a small peak corresponding to the hydronium ion is measured at  $m/z$  19.

Other primary peaks at  $m/z$  57, 85, 103, 147, 161, 175, 189, 203, 217, 231, 245 and 259 were detected in the positive mass spectrum. Peak assignments and proposed structures for these primary peaks associated with bond scission and recombination are shown in tables 1 and 2. Besides the primary peaks assigned to bond scission are associated a series of smaller mass peaks which correspond to loss of hydrogen. These peaks can account for a loss of up to 8 hydrogen atoms from the main ion fragment. Interestingly, the peaks associated with a loss of an even number of hydrogen atoms are more intense than those corresponding to loss of an odd number of hydrogen atoms. For instance, the protonated precursor peak was observed at  $m/z$

131 with minor peaks at 129 and 127 m/z. The peaks at 130 and 128 m/z were either very low in intensity or not observed at all.

#### ETMA/D<sub>2</sub>O

Figure 5 shows the positive ion mass spectrum for a (1:1) mixture of ETMA and D<sub>2</sub>O at input power of 10 W and total pressure of 0.06 mbar. The peak at m/z 132 corresponds to the deuterated precursor molecule [M+D]<sup>+</sup>. The peak corresponding to the hydronium ion for ETMA/H<sub>2</sub>O plasma appears at m/z 21 and 22, corresponding to HD<sub>2</sub>O<sup>+</sup> and D<sub>3</sub>O<sup>+</sup> respectively. The spectrum shows similar peaks which correspond to the peaks for ETMA/H<sub>2</sub>O but shifted to higher m/z as H<sup>+</sup> is replaced with D<sup>+</sup>. For example, the peak at m/z 103 for ETMA/H<sub>2</sub>O corresponding to loss of an ethyl group is shifted to m/z 104 for ETMA/D<sub>2</sub>O.

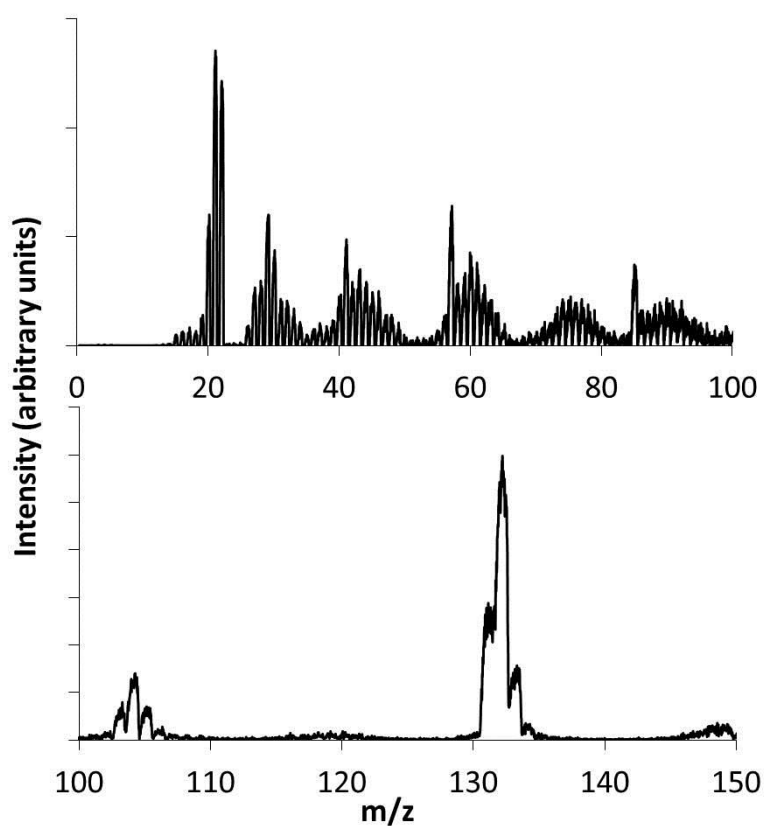


Figure 5 Positive ion mass spectrum of ETMA/D<sub>2</sub>O plasma at 0.06 mbar and 10W

#### Discussion

Hydrogen in the plasma chamber may be in the form of a proton (H<sup>+</sup>), atomic hydrogen (H•) or covalently bound hydrogen (H). The chemistry of hydrogen in the plasma determines its stability, charge and mobility, which are all important considerations in how hydrogen interacts

with other species in the plasma phase. As we will discuss, the chemistry of an individual hydrogen atom can change many times during its residence time in the plasma chamber due to interactions in the plasma and thus the roles hydrogen plays are interrelated.

### **Chemistry of H in the plasma phase**

Precursor molecules (ETMA and H<sub>2</sub>O) enter the chamber intact and may undergo ionisation and fragmentation due to collisions with high energy electrons. RF energy required to initiate these processes couples with free electrons which are heated, resulting in a distribution of electron energies in the plasma from low energy electrons (~1eV) up to >10eV, with a typical average electron energy of 3eV. Electrons are capable of causing different reactions with neutral molecules depending on their energy, including ionisation, dissociation and elastic scattering reactions. The energy of the collision then may determine the nature of hydrogen in the plasma phase. From the OES and MS data, there are 3 forms of H in the plasma phase.

(1) As shown by MS in Fig 4, there are many ETMA precursor fragments and oligomers which retain their hydrocarbon structure, and the peak at 19m/z represents protonated water. Therefore, H is present in the plasma which is covalently bonded to either ETMA Carbon atoms or Water Oxygen atoms. A minor amount of covalently bonded H<sub>2</sub> may also be present as shown by OES, and this may be either excited or at ground state.

(2) Electron collisions with precursor molecules may result in abstraction of H• if the electron energy is approximately 3-5eV. While these species cannot be detected by MS as they are uncharged, H• can be observed in the plasma by OES which shows characteristic H<sub>α</sub> and H<sub>β</sub> peaks. As expected, the density of H• increases as the applied power increases and the density of electrons increases.

(3) Finally, H<sup>+</sup> exist in the plasma phase as shown by MS which exhibits peaks corresponding to protonated precursor molecules. H<sup>+</sup> may be formed by high energy electron collisions, greater than ~10eV, with atomic hydrogen.<sup>40</sup> Note that while individual H<sup>+</sup> are charged, they cannot be measured using the Hiden as the instrument sensitivity at small m/z is very low. Protonated species are however evident at 131 m/z [ETMA + H]<sup>+</sup> and 19 m/z [H<sub>3</sub>O]<sup>+</sup>.

H which is covalently bonded to Carbon or Oxygen is by definition quite stable in the plasma, and is generally unreactive unless activated by electron collisions; however H• and H<sup>+</sup> are thermodynamically unstable and therefore quite reactive.<sup>41,42</sup>

## Precursor Fragmentation, Protonation and Abstraction of Hydrogen

The positive ion mass spectra of ETMA plasmas show peaks which correspond to homolytic cleavage of C-C or C-O bonds, and protonation. The formation of these ionic fragments is summarised in Table 1. Loss of a methyl group (from either the acid or alcohol side of the precursor) results in a radical with a molecular weight of 115 amu, which after radical quenching with H• and protonation should appear as a peak at 117m/z. This peak is observed but with only minor intensity compared to the peak at 103 m/z which results from loss of the ethyl group via scission of the C-O bond. This indicates that the C-C ethyl bond is more stable than the ester C-O bond in ETMA. This may be due to the ester C-O bond strength being lower than the C-C,<sup>43</sup> or due to shielding of the C-C bond from electrons by covalently bound H. It also suggests that the tert-butyl group remains stable, as degradation of the tert-butyl group would entail sequential loss of methyl groups which is only observed at low intensity.

Similarly, loss of the intact tert-butyl group would result in a species with molecular weight 73 amu, and a protonated peak at 75 m/z; this peak is observed in Fig 4, but only at very low intensity. In contrast, the peak at 57 m/z corresponding to scission of the tert-butyl group is relatively intense. This indicates a higher stability of the tert-butyl ion compared to the ester. While the ester group can resonance stabilise a proton, the stability of carbonium ions is significantly increased by attachment to other carbon atoms.<sup>44</sup>

The spectra also exhibit ionic species larger than the precursor, with primary peaks including 203 and 259 m/z. The 259 m/z peak corresponds to the dimer [2M-H]<sup>+</sup> and results from the loss of H• from two precursor molecules resulting in the formation of two radicals which recombine to form a molecule with a weight of 258 amu. This species can then be protonated to form the 259 m/z peak. Subsequent replacement of methyl groups with H• results in peaks at 245, 231 and 217m/z. Similar radical formation can occur through scission of a C-C bond. For example, loss of a single H• from one precursor (129 amu) and loss of the tert-butyl group from another (73 amu) results in formation of a 202 amu species after recombination, which is then protonated to form the 203 m/z peak. Again, replacement of methyl groups with H• gives rise to peaks at 189 and 175m/z. Loss of the tert-butyl group from two precursors followed by recombination and protonation gives rise to the peak at 147 m/z.

For each of the primary peaks mentioned above, there exists a series of peaks offset by 2 m/z. Peaks at -1, -3 etc m/z are only observed at very low intensity indicating these species are unstable compared to the peaks offset by an even m/z.

## Source of protonation

The positive ion mass spectra of ETMA/H<sub>2</sub>O plasmas show a protonated precursor peak [M+H]<sup>+</sup> at 131m/z, and other protonated species. This is in contrast to the RGA spectra which show the ionised precursor peak at 130 m/z. This indicates that electron impact and removal of an electron is not the primary mechanism of ionisation in the plasma phase. The mechanism for protonation may be due to hydrogen in the form of free protons (H<sup>+</sup>) in the plasma phase, or proton transfer from species with lower proton affinities. There are two possible sources of hydrogen being delivered to the plasma chamber; the ETMA precursor and water. As the partial vapour pressures of water and ETMA are the same in Fig 4 (both 0.03 mbar) the number of ETMA and water molecules must be equal. Each ETMA molecule has 14 H atoms, while water has 2. Therefore 7 times as much H is supplied to the chamber from ETMA as from water. In addition, the bond strength of HO-H is higher than C-H, at 493 kJ/mol and ~420 kJ/mol respectively.<sup>43</sup> Thus, when high energy electrons in the plasma collide with precursor molecules, they are more likely to abstract H• from ETMA than water. The bond dissociation energy of D<sub>2</sub>O and H<sub>2</sub>O remains virtually unchanged,<sup>45</sup> and so we would expect the same to be true for ETMA/D<sub>2</sub>O plasmas; in this case, there would be far more H• in the plasma phase than atomic deuterium (D•).

Thus, if free H•/D• was the main source of protonation of the ETMA precursor in the plasma, in both cases a dominant peak at [M+H]<sup>+</sup> should be observed, with only a minor peak [M+D]<sup>+</sup> for ETMA/D<sub>2</sub>O plasma. However the mass spectrum for ETMA/D<sub>2</sub>O plasma shows a dominant peak at 132 m/z, corresponding to the deuterated precursor, with a smaller peak at 131 m/z assigned to the protonated precursor. Therefore the main source of protons must not be free H•.

The formation of hydronium (H<sub>3</sub>O<sup>+</sup>) is well known in astrophysics and is independent of temperature above approximately 10K.<sup>46</sup> There are a number of reactions in the plasma phase which lead to hydronium formation, including:



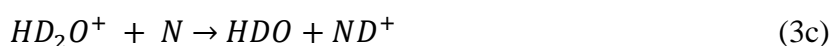
All of these reactions require multiple collisions (i.e. formation of H<sub>2</sub><sup>+</sup> or H<sub>2</sub>O<sup>+</sup> first) but have relatively high rate constants in the gas phase.<sup>47</sup> Molecule and ion formation is also possible due to H atoms impacting surfaces,<sup>48</sup> however this mechanism is only found to be important at very low (interstellar) pressures.

It has previously been postulated that  $H_3O^+$  may be a source of protonation in the plasma phase by transfer of  $H^+$  to a neutral molecule, as shown in Equation 2, providing the proton affinity of the neutral is higher than water<sup>35</sup>:



The proton affinity for water is 697 kJ/mol, while acetates are generally in the region of 800-850 kJ/mol, and thus proton transfer is a likely route for protonation.<sup>49,50</sup>

The mass spectra for  $D_2O$  and ETMA/ $D_2O$  plasmas show peaks at 21 and 22m/z, corresponding to  $HD_2O^+$  and  $D_3O^+$ . If  $H_3O^+$  were replaced by  $HD_2O^+$  and  $D_3O^+$  in equation 2, then we can write modified equations as below:



Therefore assuming the affinity for  $H^+$  and  $D^+$  is similar, if the source of protonation for ETMA is protonated water, we should observe greater intensity at 132 m/z  $[M+D]^+$  compared to 131 m/z  $[M+H]^+$ . This is what is observed, and shows that  $H^+$  transfer from water is the most likely route to protonation in the plasma phase. To support this hypothesis, experiments were performed with (1:2) and (2:1) ratios of ETMA/ $D_2O$  in the plasma, and the positive ion mass spectra of the protonated precursor measured. The results in figure 6 show that increasing the amount of  $D_2O$  in the plasma increases the relative abundance of  $[M+D]^+$ . For the experiments performed here, water has been deliberately added to the chamber, but it should be noted that in our experience it is virtually impossible to remove all water from the chamber walls and a protonated water peak at 19 m/z is always observed.

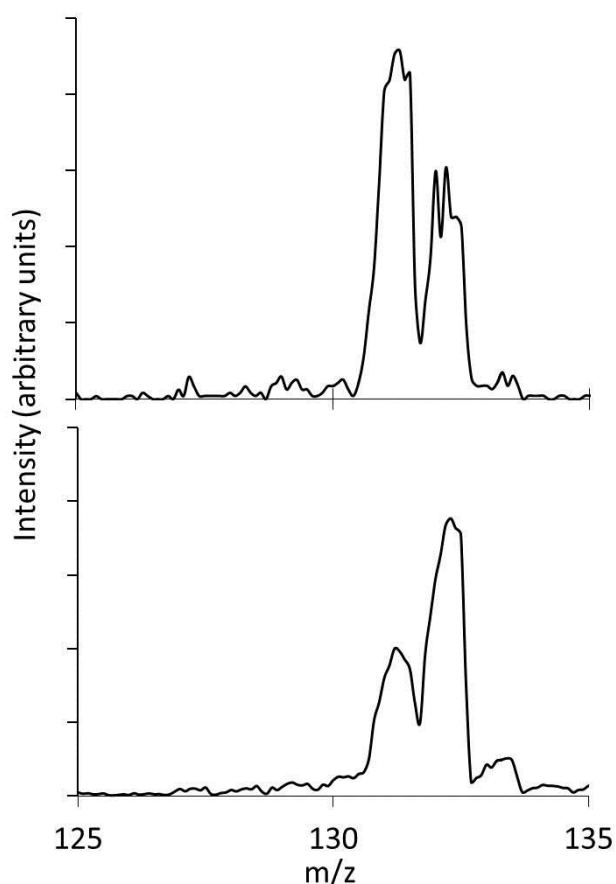
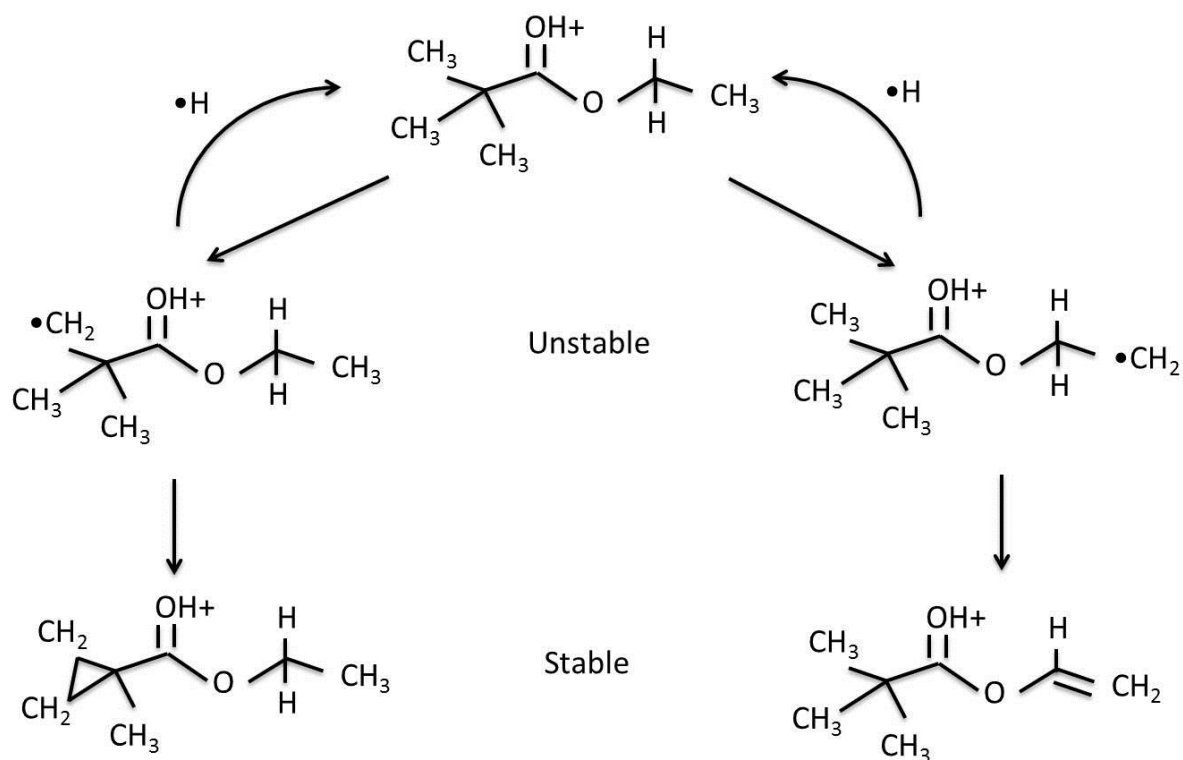


Figure 6. Positive ion mass spectra of the protonated precursor in ETMA/D<sub>2</sub>O plasma at 0.06 mbar and 10W. 2 ETMA : 1 D<sub>2</sub>O (top) and 1 ETMA : 2 D<sub>2</sub>O (bottom)

### Radical formation, quenching and substitution

As shown in figure 4, a series of daughter peaks for each primary peak were identified in ETMA/H<sub>2</sub>O plasma which are offset by -2, -4, -6 amu. For example, the protonated precursor at m/z 131 is associated with smaller peaks at m/z 129 and 127. With abstraction of a single H• from the protonated ETMA precursor, an ionic radical is formed which is inherently unstable due to the unpaired electron remaining. Peaks which are offset by -1, -3 amu are very low in intensity, confirming these species are unstable and present in only very low densities in the plasma. There are then two reactions which can lead to quenching of this radical and stabilisation of the protonated species as shown in Scheme 1; combination with another radical in the plasma phase, or self-quenching by abstraction of another neighbouring H•.





Scheme 1. Mechanisms of abstraction of hydrogen, radical quenching and recombination.

Abstraction of  $\text{H}\cdot$  and formation of a radical centre leads to weakening of neighbouring C-H bonds.<sup>43</sup> For example, it has been shown that  $\beta\text{C-H}$  bonds are reduced in strength by approximately 2/3. Therefore, after initial abstraction of  $\text{H}\cdot$ , the probability of neighbouring  $\text{H}\cdot$  being abstracted by electron collisions is increased. Removal of another  $\text{H}\cdot$  and radical formation would then enable the two radical centres to quench, forming a new C-C bond, and a stable ion with a mass reduced by 2 amu. The nature of this bond would depend on the positions of the carbon atoms in the structure of the ion; if abstraction occurred on the alcohol side of the ester, it would result in formation of a double bond. If this occurred on the acid side of ETMA, it would result in the formation of a saturated cyclic prop-alkyl structure. This process could then be repeated as long as pairs of neighbouring H exist in the ion structure. Thus, in the context of deposition, the series of daughter peaks results in stable ions which may deposit by ion impact, but also possibly by radical propagation via a newly formed double bond.

Alternatively, radical quenching may be the result of combination with other plasma phase radicals. From the OES and MS results, possible radical species in the plasma phase include  $[\text{ETMA-H}]^\cdot$ ,  $[\text{ETMA-C}_2\text{H}_5]^\cdot$ ,  $(\text{CH}_3)_3\text{C}\cdot$ , and  $\text{H}\cdot$ . The probability of recombination with each

of these species is dependent on several factors including their density in the plasma, mobility and orientation effects.

In the bulk of plasma only the electrons are heated, while ions neutrals and radicals all remain close to ambient temperature.<sup>51</sup> Therefore the thermal velocity of particles within the bulk of the plasma is given by equation 3:<sup>52</sup>

$$v = \sqrt{\frac{8kT}{m\pi}} \quad (3)$$

where  $k$  is Boltzmann's constant,  $T$  is the absolute temperature and  $m$  is the mass of the particle. Assuming that the atoms and molecules in the plasma phase remain at  $\sim 300\text{K}$ , the velocities of some typical radical species in ETMA plasmas can be calculated to be  $\text{H}\cdot$  2520 m/s,  $(\text{CH}_3)_3\text{C}\cdot$  333 m/s  $[\text{ETMA-C}_2\text{H}_5]\cdot$  248 m/s and  $[\text{ETMA-H}]\cdot$  221 m/s. While it is difficult to determine the relative densities of each of these radical species in the plasma phase, the OES data shows that  $\text{H}\cdot$  is certainly present and is approximately 7-10 times more mobile than other radical species. In addition, as  $\text{H}\cdot$  is spherical the unpaired electron is always available despite orientation, unlike larger radical species,  $[\text{ETMA-H}]\cdot$  for example. Thus, abstracted  $\text{H}\cdot$  is likely to be replaced by  $\text{H}\cdot$  from the plasma very quickly, and protonated species returned to their original  $m/z$ . This is supported by the appearance of peaks  $m/z$  245, 231 and 217, the result of loss of methyl groups from the  $[\text{2M-H}]^+$  dimer. Loss of a methyl group would result in a loss of mass of 15 amu and formation of a radical. However these peaks are offset by 14amu, showing that the radical is quickly quenched by  $\text{H}\cdot$ , forming a stable ion.

This is also demonstrated by the MS results for ETMA:/D<sub>2</sub>O plasmas. In this case, abstracted  $\text{H}\cdot$  could be replaced by either  $\text{H}\cdot$  or  $\text{D}\cdot$  from the plasma. If abstracted  $\text{H}\cdot$  is replaced by  $\text{D}\cdot$ , then an increase of 1 amu would be observed. A comparison of the MS of the tert-butyl carbonium ion and daughter peaks with H<sub>2</sub>O and D<sub>2</sub>O in the plasma is given in Fig 7 and shows the largest ion for ETMA/H<sub>2</sub>O plasma is the  $(\text{CH}_3)_3\text{CH}_2^+$  species at 59  $m/z$ . For D<sub>2</sub>O plasma though, peaks between 59 - 64  $m/z$  are observed, showing that up to 5 of 11 H atoms are replaced with  $\text{D}\cdot$ . Similar series are observed for other primary peaks in the MS of ETMA/D<sub>2</sub>O plasma. As was noted above, there is 7 times more  $\text{H}\cdot$  than  $\text{D}\cdot$  in the plasma, so it likely that most radical quenching is due to simply replacing  $\text{H}\cdot$ , or even  $\text{D}\cdot$  being replaced with  $\text{H}\cdot$ . Therefore in order to replace 5 H atoms with  $\text{D}\cdot$  probably takes many more abstraction/substitution reactions. This surprising result shows there is a constant exchange of H between organic molecules in the gas phase of plasmas which has not been considered previously.

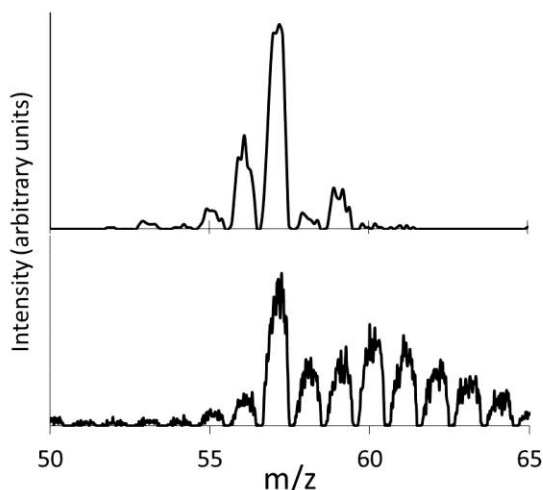


Figure 7. Positive ion mass spectra of tert-butyl ion for ETMA/H<sub>2</sub>O (top) and ETMA/D<sub>2</sub>O (bottom) plasma.

### Implications for depositing organic plasmas

Previously it has been shown that the chemistry of the precursor affects the relative roles of ionic deposition versus deposition via radical routes<sup>13</sup>. For saturated precursors, ions may account for up to 50% of the deposition, while unsaturated precursors are typically dominated by radical propagation. What has been less clear is how the chemistry of the precursor changes once molecules enter the plasma phase; MS results have helped to give a snapshot of plasma chemistry, but the dynamics of the physico-chemical processes have largely been ignored. The results and discussion above demonstrate that organic molecules in depositing plasmas constantly undergo a series of reactions; H<sup>+</sup> transfer from hydronium, fragmentation via C-C or C-O bond scission, H• abstraction and radical recombination. Hydrogen plays a key role in many of these processes due to its abundance in the plasma and its relatively high mobility. Hydrogen is important in activating plasma species by protonation, which are then accelerated to surfaces immersed in the plasma due to the development of negative surface potentials.<sup>51</sup> This increases the flux of ions to the surface by approximately 15 times compared to neutral species of the same density, and enables them to gain significant kinetic energy on approach to the surface. This kinetic energy (typically 10-30eV) is enough to facilitate deposition. Abstraction of H• also activates plasma species by creating radical centres which can react with other plasma phase radicals or surface radicals.

However H• also plays a role in deactivating plasma species by radical quenching. As shown by the replacement of H• with D•, this process is very dynamic with H being constantly exchanged between organic molecules in the plasma, and thus quenching radicals very quickly

as they are formed. As noted by Peter et al, free H• also decreases the deposition rate by quenching surface radicals, leaving fewer reactive surface sites available for interfacial covalent bond formation with radical species arriving from the plasma phase.<sup>1</sup> The role of H• in plasma phase radical quenching was demonstrated by Dilks and Kay,<sup>53</sup> who studied plasma deposition of ethylene and a series of fluoroethylenes. XPS analysis showed that the films were depleted of F, and that part of the reason for this was many of the plasma species had increased ratio of H:F compared to the precursor. Therefore when a relatively large (and slow) F atom was abstracted, it was more likely to be replaced with the highly mobile H•. Vasile and Smolinsky also observed that fluoroethylenes exhibit higher polymerisation in the plasma than ethylene, which may be explained by the radical species having a shorter lifetime when H• is abundant in the plasma;<sup>54</sup> longer lived fluorinated ethylene radicals have increased probabilities of quenching with other fluorinated ethylene radicals rather than with H•.

It has also been observed in the plasma deposition of many organic compounds that H is depleted in the film. For example, methane is 80 at% H, however plasma deposits of methane gas are typically ~30 at% H.<sup>1,18</sup> In this case, abstraction of H• results in H<sub>3</sub>C• which can react with surface radicals in order to deposit. Abstraction of a single H• is not enough to explain the low H content in these films though, and so di- and even tri-radical carbons must be formed in the plasma phase, which may result in unsaturation when incorporated into the film. Similarly, Peter et al measured the H content of C<sub>2</sub>H<sub>2</sub> plasma deposits well below the stoichiometry of the precursor at 50 at%.<sup>1</sup> MS analysis of the positive ions revealed strong peaks at 50 and 74 m/z corresponding to C<sub>4</sub>H<sub>2</sub><sup>+</sup> and C<sub>6</sub>H<sub>2</sub><sup>+</sup> which are severely depleted of H and contain additional C=C bonds which are induced by the plasma. Indeed, for larger organic precursors, near edge X-ray absorption fine structure (NEXAFS) has been utilised to measure unsaturation in films generated from allylamine, propylamine, ethylene and diethylene glycol dimethyl ether.<sup>32-34</sup> While some of these precursors contain unsaturated carbon in their structure (e.g. allylamine and ethylene), methane, propylamine and diethylene glycol dimethyl ether do not but still exhibit unsaturation when deposited via plasma. In all cases, the level of unsaturation increased with applied power. The findings here point to unsaturation being due to plasma phase abstraction of neighbouring H• and radical self-quenching, and this phenomenon would increase as the electron temperature and density are increased with applied power.

Thus, the chemistry of thin films from polymerising plasmas is linked to the chemistry of the plasma phase, and hydrogen plays a key role in many of the chemical processes in the plasma.

## Conclusion

Hydrogen plays multifaceted roles in plasma. The results presented here show that  $H^+$  transfer from hydronium is a key mechanism for ionising plasma precursors, and that electron impacts generally result in bond scission and precursor fragmentation, but are less important in ionisation. This result is important as even under high vacuum, residual water physisorbed to the chamber walls becomes the dominant species for determining ionisation processes. Hydrogen is then important in activating precursor ions and providing them with sufficient kinetic energy to deposit.

Abstraction of  $H\cdot$  is also an important process, activating precursor molecules by producing radicals and liberating  $H\cdot$  into the plasma. These radical species are inherently unstable and MS results indicate they are short lived due to radical quenching. One route to stabilising radicals is via double abstraction of  $H\cdot$  and self-quenching, resulting in formation of double bonds. This explains the unsaturation and auto-fluorescence often observed in plasma polymer films, even when the precursor is saturated. Another route to radical stabilisation is oligomerisation resulting in species larger than the precursor, but the high mobility and reactivity of  $H\cdot$  makes it the dominant species for radical quenching. By adding deuterium to the plasma, we have demonstrated that  $H\cdot$  and radical quenching is a far more dynamic process than previously thought. The result is that hydrogen is continuously being abstracted and substituted in precursor molecules throughout their residence time in the plasma chamber. These new insights into the key roles hydrogen plays in organic plasma chemistry will enable further development of mechanistic deposition models, and facilitate control and tailoring of plasma deposition processes.

## Acknowledgement

The authors wish to acknowledge financial support from the Australian Research Council under ARC Discovery Project DP160105001.

## References

1. S. Peter, K. Graupner, D. Grambole, F. Richter, *J. Appl. Phys.*, 2007, **102**, 053304
2. G. Mishra, C.D. Easton, G.J.S. Fowler, S.L. McArthur, *Polymer*, 2011, **52**, 1882-1890

3. H. Testrich, H. Rebl, B. Finke, F. Hempel, B. Nebe, J. Meichsner, *Materials Science and Engineering C*, 2013, **33**, 3875–3880
4. T.R. Gengenbach, R. Chatelier, H.J. Griesser, *Surf. Interface Anal.*, 1996, **24**, 271-281
5. S. Saboohi, B.R. Coad, H.J. Griesser, A. Michelmore, R.D. Short, *Phys. Chem. Chem. Phys.*, 2017, **19**, 5637-5646.
6. K. Ostrikov, H. Mehdipour, *J. Am. Chem. Soc.* 2012, **134**, 4303–4312
7. H. Mehdipour, K. Ostrikov, *J. Am. Chem. Soc.*, 2013, **135**, 1912–1918
8. T. Williams, M.W. Hayes, *Nature*, 1966, **209**, 769-773.
9. A.R. Denaro, P.A. Owens, A. Crawshaw, *Eur. Polym. J.*, 1969, **5**, 471-482
10. A.R. Westwood, *Eur. Polym. J.*, 1971, **7**, 363-375
11. D. Hetemi, J. Pinson, *Chem. Soc. Rev.*, 2017, **46**, 5701-5713
12. M. Moreno-Couranjou, A. Manakhov, N.D. Boscher, J.J. Pireaux, P. Choquet, *ACS Appl. Mater. Interfaces*, 2013, **5**, 8446-8456
13. A. Michelmore, P. Gross-Kosche, S.A. Al-Bataineh, J.D. Whittle, R.D. Short, *Langmuir*, 2013, **29**, 2595-2601.
14. A. Choukourov, O. Kylián, M. Petr, M. Vaidulych, D. Nikitin, J. Hanuš, A. Artemenko, A. Shelemin, I. Gordeev, Z. Kolská, P. Solař, I. Khalakhan, A. Ryabov, J. Májek, D. Slavínská, H. Biederman, *Nanoscale*, 2017, **9**, 2616-2625
15. A. Michelmore, D.A. Steele, D.E. Robinson, J.D. Whittle, R.D. Short, *Soft Matter*, 2013, **9**, 6167-6175
16. K. Bazaka, J. Ahmad, M. Oelgemöller, A. Uddin, M.V. Jacob, *Sci. Rep.*, 2017, **7**, 45599
17. M.V. Jacobs, C.D. Easton, G.S. Woods, C.C. Berndt, *Thin Solid Films*, 2008, **516**, 3884
18. D.L. Pappas, J. Hopwood, *J. Vac. Sci. Technol. A*, 1994, **12**, 1576
19. F. Khelifa, S. Ershov, Y. Habibi, R. Snyders, P. Dubois, *Chem. Rev.*, 2016, **116**, 3975–4005
20. T.D. Michl, B.R. Coad, M. Doran, M. Osiecki, M.H. Kafshgari, N.H. Voelcker, A. Hüsler, K. Vasilev, H.J. Griesser, *Chem. Commun.*, 2015, **51**, 7058-7060
21. K. Vasilev, V. Sah, K. Anselme, C. Ndi, M. Mateescu, B. Dollmann, P. Martinek, H. Ys, L. Ploux, H.J. Griesser, *Nano Lett.*, 2010, **10**, 202–207
22. S.W. Tsai, M. Loughran, A. Hiratsuka, K. Yano, I. Karube, *Analyst*. 2003, **128**, 237-44.
23. E. Körner, G. Fortunato, D. Hegemann, *Plasma Processes Polym.*, 2009, **6**, 119-125
24. A. Choukourov, H. Biederman, D. Slavinska, L. Hanley, A. Grinevich, H. Boldryeva, A. Mackova, *J. Phys Chem. B*, 2005, **109**, 23086-23095

25. F. Khelifa, S. Ershov, Y. Habibi, R. Snyders, P. Dubois, *ACS Appl. Mater. Interfaces*, 2013, **5**, 11569–11577
26. D. Bohm, In *The Characteristics of Electrical Discharges in Magnetic Fields*; A. Guthrie, R.K. Wakerling, Eds.; McGraw Hill: New York and London, 1949.
27. D.C. Jacobs, *Annu. Rev. Phys. Chem.* 2002, **53**, 379–407.
28. A. von Keudell, *Plasma Sources Sci. Technol.*, 2000, **9**, 455–467.
29. G.P. Wells, I.C. Estrada-Raygoza, P.L.S. Thamban, C.T. Nelson, C. –W. Chung, L.J. Overzet, M.J. Goeckner, *Plasma Processes Polym.*, 2013, **10**, 119–135
30. S. Saboohi, B.R. Coad, A. Michelmore, R.D. Short, H.J. Griesser, *ACS Appl. Mater. Interfaces*, 2016, **8**, 16493-16502
31. L. O'Toole, A.J. Beck, R.D. Short, *Macromolecules*, 1996, **29**, 5172-5177
32. S. Swaraj, U. Oran, A. Lippitz, R-D. Schulze, J.F. Friedrich, W.E.S. Unger, *Plasma Process. Polym.* 2005, **2**, 310-318
33. G. Alexander, A.G. Shard, J.D. Whittle, A.J. Beck, P.N. Brookes, N.A. Bullett, R.A. Talib, A. Mistry, D. Barton, S.L. McArthur, *J. Phys. Chem. B* 2004, **108**, 12472
34. D.J. Menzies, B. Cowie, C. Fong, J.S. Forsythe, T.R. Gengenbach, K.M. McLean, L. Puskar, M. Textor, L. Thomsen, M. Tobin, B.W. Muir, *Langmuir*, 2010, **26**, 13987-13994.
35. C.A. Mayhew, R.D. Short, *Chem Commun.*, 2009, **6**, 659-661
36. A. Michelmore, J.D. Whittle, R.D. Short, R. W. Boswell, C. Charles, *Plasma Processes Polym.* 2014, **11**, 833-841
37. W. Swan, *Transactions of the Royal Society of Edinburgh*, 1857, **21**, 411
38. M. Heintze, M. Magureanu, M. Kettlitz, *J. Appl. Phys.*, 2002, **92**, 7022
39. R. Celiberto, R. K. Janev, A. Laricchiuta, M. Capitelli, J. M. Wadehra, D. E. Atems, *At. Data Nucl. Data Tables*, 2001, **77**, 161–213
40. I.C. Percival, *Nuclear Fusion*, 1966, **6**, 182-187
41. A.G. Vandeputte, M.K. Sabbe, M.-F. Reyniers, V. Van Speybroeck, M. Waroquier, G.B. Marin, *J. Phys. Chem. A* 2007, **111**, 11771-11786
42. J.J. Fifen, Z. Dhaouadi, M. Nsangou, *J. Phys. Chem. A*, 2014, **118**, 11090–11097
43. S.J. Blanksby, G.B. Ellison, *Acc. Chem. Res.*, 2003, **36**, 255-263
44. D. Bethell, V. Gold, *Quarterly Reviews*, 1958, **12**, 173-203
45. O.V. Boyarkin, M.A. Koshelev, O. Aseev, P. Maksyutenko, T.R. Rizzo, N.F. Zobov, L. Lodi, J. Tennyson, O.L. Polyansky, *Chem. Phys. Lett.*, 2013, **14–20**, 568
46. J.M. Hollis, E.B. Churchwell, E. Herbst, De Lucia, *Nature*, 1986, **322**, 524 - 526

47. M. Jimenez-Redondo, E. Carrasco, V.J. Herrero, I. Tanarro, *Plasma Sources Sci. Technol.*, 2015, **24**, 015029
48. O. Gabriel, D. C. Schram, R. Engeln, *Phys. Rev. E*, 2008, **78**, 016407
49. E.P. Hunter, S.G. Lias, *J. Phys. Chem. Ref. Data*, 1998, **27**, 413-656.
50. J. Evans, G. Nicol, N. Munson, *J Am Soc Mass Spectrom*, 2000, **11**, 789–796
51. M.A. Lieberman, A.J. Lichtenberg, *Principles of Plasma Discharges and Materials Processing*; John Wiley and Sons: Chichester, 1994
52. B. Chapman, *Glow Discharge Processes*; John Wiley and Sons: Chichester, 1980.
53. A. Dilks, E. Kay, *Macromolecules*, 1981, **14**, 855-862
54. M.J. Vasile, G. Smolinsky, *J. Phys. Chem.*, 1977, **81**, 2605–2609



## Table of Contents Graphic

